

## Double Targeting of Tumours with Pyrenyl-Modified Dendrimers Encapsulated in an Arene–Ruthenium Metallaprism

Anaïs Pitto-Barry,<sup>[a]</sup> Nicolas P. E. Barry,<sup>[a]</sup> Olivier Zava,<sup>[b]</sup> Robert Deschenaux,<sup>[a]</sup> Paul J. Dyson,<sup>[b]</sup> and Bruno Therrien\*<sup>[a]</sup>

**Abstract:** The self-assembly of 2,4,6-tris(pyridin-4-yl)-1,3,5-triazine (tpt) triangular panels with *p*-cymene–ruthenium building blocks and 5,8-dioxido-1,4-naphthoquinonato (donq) bridges, in the presence of pyrenyl-containing dendrimers of different generations ( $P_0$ ,  $P_1$  and  $P_2$ ), affords the triangular prismatic host–guest compounds  $[P_n\text{C}Ru_6(p\text{-cymene})_6(\text{tpt})_2(\text{donq})_3]^{6+}$  ( $[P_n\text{C}1]^{6+}$ ). The host–guest nature of these systems, with the pyrenyl moiety being encapsulated in the hydrophobic

cavity of the cage and the dendritic functional group pointing outwards, was confirmed by NMR spectroscopy ( $^1\text{H}$ , 2D and DOSY). The host–guest properties of these systems were studied in solution by NMR and UV/Vis spectroscopic methods, allowing the determination of their affinity constants

( $K_a$ ). Moreover, the ability of these water-soluble host–guest systems to carry the pyrenyl-containing dendrimers into cancer cells was evaluated on human ovarian cancer cells. The host–guest systems are all more cytotoxic than the empty cage  $[1][\text{CF}_3\text{SO}_3]_6$  ( $\text{IC}_{50} \approx 4 \mu\text{M}$ ), with the most active compound,  $[P_0\text{C}1][\text{CF}_3\text{SO}_3]_6$ , being an order of magnitude more cytotoxic.

**Keywords:** antitumor agents • dendrimers • drug delivery • host–guest systems • metallaprisms

### Introduction

Hypervascularity and the defective vascular architecture of the endothelial layer of blood vessels contribute to the enhanced permeability of cancer cells.<sup>[1]</sup> In addition to this enhanced vascular permeability of tumours, the lymphatic drainage system is substantially modified in cancer cells, and it appears that it does not operate efficiently.<sup>[2]</sup> Consequently, macromolecular drugs and large vectors are retained in the tumour interstitium for longer periods than in healthy tissues. The combination of poor tissue drainage and increased tumour vascular permeability results in a phenomenon termed the enhanced permeability and retention

(EPR) effect. This effect is believed to play a major role in the selectivity of nanomedicines towards cancer cells, which causes an intratumour drug delivery efficacy up to 100 fold greater than that observed in healthy cells.<sup>[3]</sup> There are many types of nanomedicine, including antibodies and polymeric drugs, but also large drug-delivery vectors, such as micelles and nanoparticles. Indeed, an EPR effect has been observed for proteins,<sup>[4]</sup> micelles composed of block copolymers,<sup>[5]</sup> encapsulated drugs,<sup>[6]</sup> liposomes,<sup>[7]</sup> and even bacteria with diameters of 1–2  $\mu\text{m}$ .<sup>[8]</sup>

We have synthesised a number of arene–ruthenium metalla-assemblies, in particular hexanuclear metallaprisms that form hexacationic cages, which potentially use the EPR effect to target cancer cells.<sup>[9]</sup> These water-soluble assemblies have been found to be active against cancer cells,<sup>[10]</sup> and their cavities have been used to encapsulate various guest molecules permanently<sup>[11]</sup> or reversibly.<sup>[12]</sup> Tetranuclear arene–ruthenium rectangles were found to be cytotoxic against human ovarian A2780 cancer cell lines,<sup>[13]</sup> and may also encapsulate guest molecules.<sup>[14]</sup> These compounds exhibit a size effect, with the smaller rectangular molecules being only moderately cytotoxic, whereas the larger are more cytotoxic ( $\text{IC}_{50} \approx 4 \mu\text{M}$ ).<sup>[13]</sup> The same size effect was observed with arene–ruthenium metallacubes incorporating different tetrapyrrolylporphyrin panels, with the larger as-

[a] A. Pitto-Barry, N. P. E. Barry, Prof. R. Deschenaux, Dr. B. Therrien  
Institut de Chimie, Université de Neuchâtel  
Avenue de Bellevaux 51, 2000 Neuchâtel (Switzerland)  
Fax: (+41)32-7182511  
E-mail: bruno.therrien@unine.ch

[b] Dr. O. Zava, Prof. P. J. Dyson  
Institut des Sciences et Ingénierie Chimique  
Ecole Polytechnique Fédérale de Lausanne (EPFL)  
1015 Lausanne (Switzerland)

Supporting information for this article is available on the WWW under <http://dx.doi.org/10.1002/chem.201002634>.

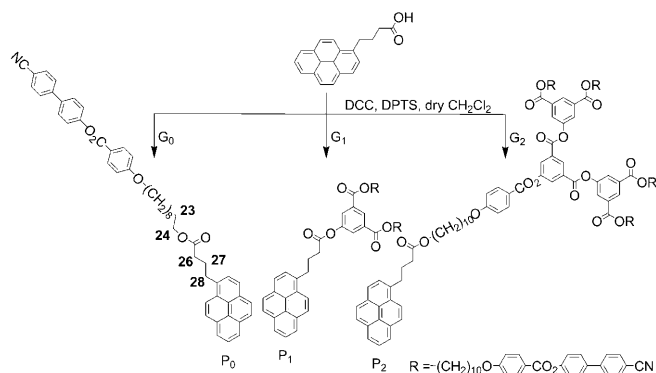
semblies being more cytotoxic than the smaller octanuclear assemblies.<sup>[15]</sup>

To determine the impact of the size of a guest, a series of large pyrenyl-containing dendrimers of different generations has been prepared (generation zero: P<sub>0</sub>, generation one: P<sub>1</sub> and generation two: P<sub>2</sub>). The pyrenyl units were encapsulated in the hydrophobic cavity of a hexanuclear arene–ruthenium cage complex [Ru<sub>6</sub>(*p*-cymene)<sub>6</sub>(tpt)<sub>2</sub>(donq)<sub>3</sub>]<sup>6+</sup> (**1**)<sup>6+</sup>; tpt = 2,4,6-tris(pyridin-4-yl)-1,3,5-triazine; donq = 5,8-dioxido-1,4-naphthoquinonato), and the cytotoxicity of these resulting host–guest systems, [P<sub>0</sub>⊂**1**]<sup>6+</sup>, [P<sub>1</sub>⊂**1**]<sup>6+</sup> and [P<sub>2</sub>⊂**1**]<sup>6+</sup>, was evaluated and correlated to their size.

## Results and Discussion

**Synthesis:** The synthesis of guest molecules P<sub>0</sub>, P<sub>1</sub> and P<sub>2</sub> involves three generations of cyanobiphenyl dendritic precursors (G<sub>0</sub>, G<sub>1</sub> and G<sub>2</sub>), the synthesis of which has been reported previously.<sup>[16]</sup> P<sub>0</sub>, P<sub>1</sub> and P<sub>2</sub> were prepared by an esterification reaction between 1-pyrenebutyric acid and the different generations of cyanobiphenyl dendrimer (see Scheme 1). Dendrimers, such as those described here, are interesting materials as their size can be controlled and adjusted precisely through a convergent synthetic methodology.<sup>[17]</sup> In the case of G<sub>2</sub>, an arm comprising an aliphatic C<sub>10</sub>H<sub>20</sub> chain was included to add flexibility to this large dendritic moiety and to increase the yield of the coupling reaction.

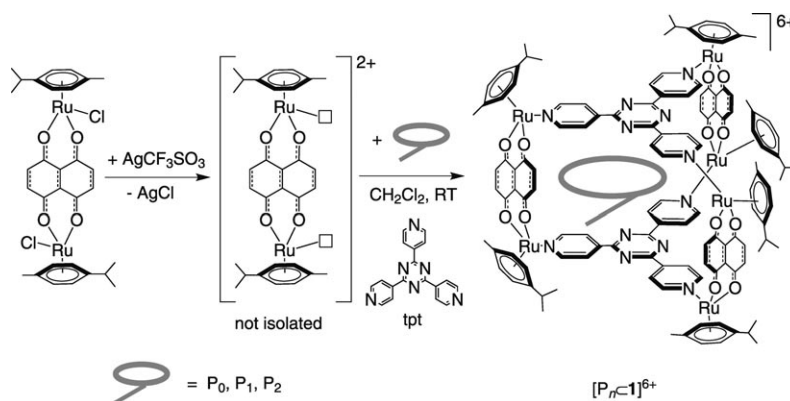
The esterification reactions were monitored by <sup>1</sup>H NMR spectroscopy, with observation of the signals of the pyrenyl protons (H<sup>26</sup>, H<sup>27</sup> and H<sup>28</sup>) as these are shifted slightly upfield (by up to 0.05 ppm relative to 1-pyrenebutyric acid) after coupling (see Scheme 1 for assignment). Additionally, a significant modification of the chemical environment of



Scheme 1. Syntheses of P<sub>0</sub>, P<sub>1</sub> and P<sub>2</sub> (DCC = *N,N'*-dicyclohexylcarbodiimide, DPTS = 4-(dimethylamino)pyridinium *para*-toluenesulfonate).

protons H<sup>23</sup> and H<sup>24</sup> of the linker unit leads to a significant upfield shift of 0.44 ppm in the case of the resonance of proton H<sup>24</sup>, and of 0.05 ppm for H<sup>23</sup>, confirming the formation of P<sub>0</sub>, P<sub>1</sub> and P<sub>2</sub>.

Encapsulation of the pyrenyl moiety into metallaprism [**1**]<sup>6+</sup> (see Scheme 2) is straightforward for P<sub>0</sub> and P<sub>1</sub>; addition of silver triflate to the dinuclear metallaclip [Ru<sub>2</sub>(*p*-



Scheme 2. Encapsulation of P<sub>0</sub>, P<sub>1</sub> and P<sub>2</sub> in metallaprism [**1**]<sup>6+</sup>.

cymene)<sub>2</sub>(donq)Cl<sub>2</sub>] in the presence of tpt panels and the guest molecule leads to the formation of [P<sub>0</sub>⊂**1**][CF<sub>3</sub>SO<sub>3</sub>]<sub>6</sub> and [P<sub>1</sub>⊂**1**][CF<sub>3</sub>SO<sub>3</sub>]<sub>6</sub>, respectively. In the case of P<sub>2</sub>, direct encapsulation necessitates 2 days and dichloromethane is required to solubilise P<sub>2</sub> to afford the desired carceplex system [P<sub>2</sub>⊂**1**][CF<sub>3</sub>SO<sub>3</sub>]<sub>6</sub>. All of the complexes are isolated as triflate salts and are highly soluble in solvents such as dichloromethane and water.

**Characterisation:** The host–guest compounds were unambiguously characterised by IR, UV and NMR spectroscopy, as well as MS spectrometry, and their purity was assessed by elemental analysis.

The IR spectra of [P<sub>*n*</sub>⊂**1**][CF<sub>3</sub>SO<sub>3</sub>]<sub>6</sub> are dominated by peaks between 1500 and 1600 cm<sup>-1</sup>, due to stretching of the C=C bonds of the tpt panels, and the C=N stretching vibrations around 1200 cm<sup>-1</sup>. The bands associated with the donq bridges, including the strong C=O stretching vibration (≈1630 cm<sup>-1</sup>), are only slightly altered compared with the dinuclear complex [Ru<sub>2</sub>(*p*-cymene)<sub>2</sub>(donq)Cl<sub>2</sub>].<sup>[12a]</sup> Moreover, strong stretching vibrations due to the triflate anions (1260(s), 1030(s) and 638(m) cm<sup>-1</sup>) are also observed in the IR spectra of these salts. Additional absorptions originating from the guest molecule are also observed, notably, a signal at 1730 cm<sup>-1</sup> corresponding to C=O stretching vibrations, signals at around 1500 cm<sup>-1</sup> assigned to valence vibrations of aromatic Csp<sup>2</sup>–Csp<sup>2</sup> centres and a characteristic signal at 2228 cm<sup>-1</sup> assigned to the C≡N triple bond in the dendritic arms.

The electronic absorption spectra of host–guest systems [P<sub>*n*</sub>⊂**1**]<sup>6+</sup> are characterised by an intense high-energy band centred at around 250 nm, probably corresponding to

ligand-localised or intra-ligand  $\pi \rightarrow \pi^*$  transitions. Broad low-energy bands associated with metal-to-ligand charge transfer (MLCT) transitions are also observed at 450 nm and between 600 and 800 nm, which is consistent with the electronic absorption spectra of metallaprism  $[1]^{6+}$ .<sup>[12a]</sup>

In the  $^1\text{H}$  NMR spectra, the resonances of protons  $\text{H}^{26}$ ,  $\text{H}^{27}$  and  $\text{H}^{28}$ , those of the different protons of the pyrenyl part of the guest molecule and of the pyridyl protons of the tpt panels are shifted upfield upon formation of the encapsulated systems  $[\text{P}_n\text{C}1]^{6+}$ , whereas the resonances of the CH protons of the bridging donq ligands are shifted downfield. The proton resonances of the *p*-cymene ligands, located at the periphery of the prism, are not significantly altered by the presence of a pyrenyl moiety in the cavity of  $[1]^{6+}$ . Similarly, the resonances of the protons located at the end of the dendritic arms are not affected following encapsulations.

Diffusion-ordered NMR spectroscopy (DOSY)<sup>[18]</sup> confirms the encapsulation of the functionalised pyrenes ( $\text{P}_n$ ) into the cavity of  $[1]^{6+}$  (see Figure 1 for the DOSY spec-

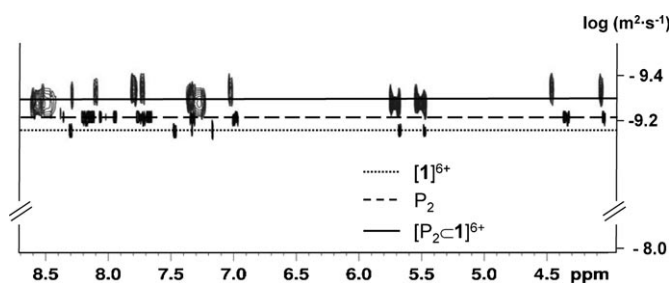


Figure 1. DOSY NMR spectra of  $\text{P}_2$ ,  $[1]^{6+}$  and  $[\text{P}_2\text{C}1]^{6+}$  in  $\text{CD}_3\text{CN}$  at  $21^\circ\text{C}$ .

trum of  $[\text{P}_2\text{C}1]^{6+}$ ). DOSY measurements of  $\text{P}_2$  ( $2871 \text{ g mol}^{-1}$ ), the empty cage  $[1]^{6+}$  ( $2457 \text{ g mol}^{-1}$ ) and the inclusion system  $[\text{P}_2\text{C}1]^{6+}$  ( $5328 \text{ g mol}^{-1}$ ) gave diffusion coefficients ( $D$ ) of  $6.16 \times 10^{-10}$ ,  $6.91 \times 10^{-10}$  and  $4.89 \times 10^{-10} \text{ m}^2 \text{ s}^{-1}$ , respectively, these values being indicative of encapsulation. The DOSY measurements of  $[\text{P}_0\text{C}1]^{6+}$  and  $[\text{P}_1\text{C}1]^{6+}$  gave similar results for these compounds. Moreover, from  $D$ , the radius ( $r$ ) of the  $[\text{P}_n\text{C}1]^{6+}$  systems was evaluated by using the Stokes–Einstein equation<sup>[19]</sup> (see Table 1).

Table 1. The molecular weight, radius and diffusion coefficients of  $\text{P}_0$ ,  $\text{P}_1$ ,  $\text{P}_2$ ,  $[1]^{6+}$ ,  $[\text{P}_0\text{C}1]^{6+}$ ,  $[\text{P}_1\text{C}1]^{6+}$  and  $[\text{P}_2\text{C}1]^{6+}$ , as determined by DOSY experiments.

	$M_w$ [ $\text{g mol}^{-1}$ ]	$r$ [ $10^{-10} \text{ m}$ ] <sup>[a]</sup>	$D$ [ $10^{-10} \text{ m}^2 \text{ s}^{-1}$ ]
$\text{P}_0$	741.91	5.25	9.33
$\text{P}_1$	1359.60	6.70	7.31
$\text{P}_2$	2871.34	7.95	6.16
$[1]^{6+}$	2600.79	7.09	6.91
$[\text{P}_0\text{C}1]^{6+}$	3342.70	7.14	6.86
$[\text{P}_1\text{C}1]^{6+}$	3960.39	8.13	6.02
$[\text{P}_2\text{C}1]^{6+}$	5472.13	10.01	4.89

[a] Radius determined by DOSY experiments.<sup>[19]</sup>

These host–guest systems were further confirmed by ESI-MS. Their mass spectra contained a peak corresponding to  $[\text{P}_n\text{C}1+(\text{CF}_3\text{SO}_3)_3]^{3+}$  at  $m/z = 1263.3$  ( $\text{P}_0$ ),  $1469.3$  ( $\text{P}_1$ ) and  $1973.5$  ( $\text{P}_2$ ).

**HyperChem simulations:** Since it was not possible to obtain an X-ray crystal structure of  $[\text{P}_0\text{C}1]^{6+}$  or the other host–guest systems, molecular modelling was performed with HyperChem software<sup>[29]</sup> to estimate the shape and size of all of these complexes in the gas phase (see Figure 2). As expect-

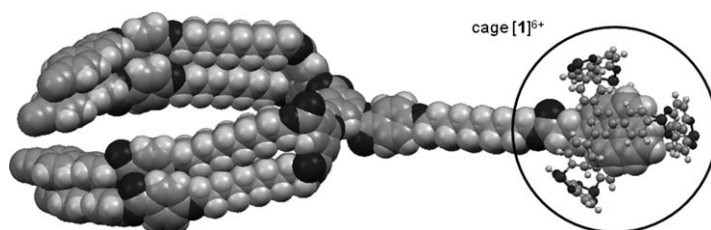


Figure 2. HyperChem simulation of the structure of  $[\text{P}_2\text{C}1]^{6+}$ , arene ligands were omitted for clarity.

ed, the HyperChem simulations show that the dendritic arm extends from the cavity with the pyrene moiety encapsulated inside the cavity of the prism. The complexes also possess two distinct regions, a hydrophilic head, consisting of the hexacationic metallacage, and a lipophilic tail, formed by the dendritic part of the complex. Such amphiphilicity is of potential relevance to the biological properties of these compounds.<sup>[20]</sup>

**Properties of the host–guest system:** The host–guest properties of the complexes were studied in solution by a combination of NMR, UV/Vis and fluorescence spectroscopy.  $^1\text{H}$  NMR titrations of  $\text{P}_0$  and  $\text{P}_1$  in the presence of  $[1]^{6+}$  were performed in  $\text{CD}_3\text{CN}$  at room temperature, whereas, in the case of  $\text{P}_2$ , broadening of the signals precludes such an analysis.

Upon gradual addition of guest  $\text{P}_0$  or  $\text{P}_1$  (0.1–3.0 equiv) to a solution of  $[1][\text{CF}_3\text{SO}_3]_6$  in  $\text{CD}_3\text{CN}$  (4.0 mM), the  $^1\text{H}$  NMR spectra show displacement of the chemical shifts of some resonances of both the host and the guest. The broadening of and change in chemical shifts of the signals support a rapid inclusion of the guest molecule into the cavity of  $[1]^{6+}$ , as observed previously with  $[\text{pyreneC}1][\text{CF}_3\text{SO}_3]_6$ .<sup>[12a]</sup> Plots of these chemical shift changes ( $\Delta\delta$ ) of the  $\beta$  proton of the tpt ligands versus the molar ratio of  $\text{P}_0$  or  $\text{P}_1$  to prism  $[1]^{6+}$  indicate a 1:1 stoichiometry of the host–guest systems (see Figure 3).<sup>[21]</sup> From these plots, stability constants of association ( $K_a$ ) were estimated by using the non-linear least-squares fitting program winEQNMR2<sup>[22]</sup> (see Table 2). The binding free energies ( $\Delta G^\circ$ ) for  $[\text{P}_0\text{C}1]^{6+}$  and  $[\text{P}_1\text{C}1]^{6+}$  were determined from the corresponding association constants obtained at  $21^\circ\text{C}$  in  $\text{CD}_3\text{CN}$  and for both  $\Delta G^\circ$  was below  $-5.80 \text{ kcal mol}^{-1}$ .

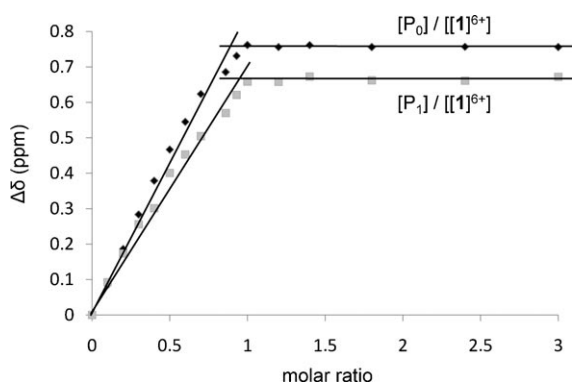


Figure 3.  $^1\text{H}$  NMR chemical shift changes for the  $\beta$  proton of the tpt ligands versus the molar ratio of  $\text{P}_0$  ( $\blacklozenge$ ) and  $\text{P}_1$  ( $\blacksquare$ ) to  $[\mathbf{1}]^{6+}$  in  $\text{CD}_3\text{CN}$  at  $21^\circ\text{C}$ .

Table 2. The association constants ( $K_a$ ) and free energies ( $\Delta G^\circ$ ) of encapsulation of  $\text{P}_0$ ,  $\text{P}_1$  and  $\text{P}_2$  in  $[\mathbf{1}]^{6+}$ , as determined by  $^1\text{H}$  NMR titration (in  $\text{CD}_3\text{CN}$  at  $21^\circ\text{C}$ , 4 mM concentration of  $[\mathbf{1}]^{6+}$ ) and by a UV/Vis method ( $\text{CH}_2\text{Cl}_2$  at  $21^\circ\text{C}$ ).

	$K_a$ [ $10^4\text{M}^{-1}$ ] <sup>[a]</sup>	$K_a$ [ $10^4\text{M}^{-1}$ ] <sup>[b]</sup>	$\Delta G^\circ$ [ $\text{kcal mol}^{-1}$ ]
$\text{P}_0 \rightarrow [\text{P}_0\text{C}\mathbf{1}]^{6+}$	4.1	7.8	-6.29
$\text{P}_1 \rightarrow [\text{P}_1\text{C}\mathbf{1}]^{6+}$	1.9	2.7	-5.83
$\text{P}_2 \rightarrow [\text{P}_2\text{C}\mathbf{1}]^{6+}$	n.a.	0.8	-5.36

[a] Determined by NMR titration; n.a. = not applicable. [b] Determined by UV/Vis spectroscopy.

Since the association constant of  $[\text{P}_2\text{C}\mathbf{1}]^{6+}$  could not be determined by NMR titration because of broadening of the signals, the association constants were also estimated by UV/Vis spectroscopy, a widely used method for the study of binding phenomena that is particularly suited to 1:1 host-guest systems.<sup>[23]</sup> Aliquots of a solution of  $[\mathbf{1}][\text{CF}_3\text{SO}_3]_6$  in  $\text{CH}_2\text{Cl}_2$  were added to a solution of the guest molecule  $\text{P}_n$  in  $\text{CH}_2\text{Cl}_2$  ( $[\mathbf{1}]/[\text{P}_n] = 0$  to 2 equiv), and the mixtures were analysed by UV/Vis spectroscopy at  $21^\circ\text{C}$ . Based on changes in the absorbance (see Figure 4 for the UV/Vis titration of

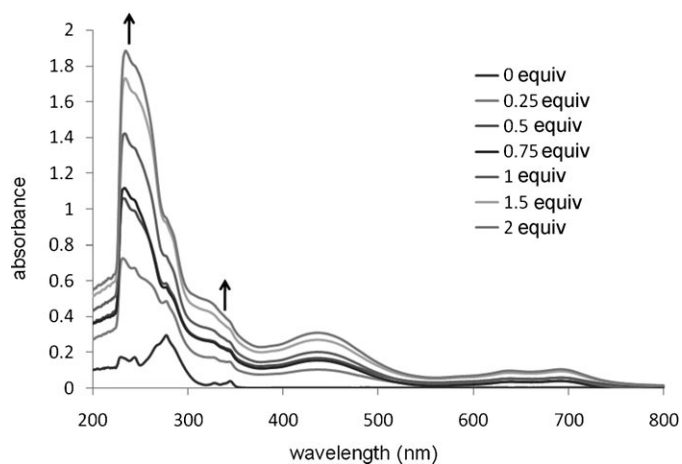


Figure 4. UV/Vis titration of  $[\mathbf{1}]^{6+}$  in a solution of  $\text{P}_2$  in  $\text{CH}_2\text{Cl}_2$  ( $10^{-5}\text{M}$ ) at  $21^\circ\text{C}$ .

$[\mathbf{1}]^{6+}$  with  $\text{P}_2$ ), and applying the Rose-Drago equation,<sup>[24]</sup> the association constants of  $[\text{P}_0\text{C}\mathbf{1}]^{6+}$ ,  $[\text{P}_1\text{C}\mathbf{1}]^{6+}$  and  $[\text{P}_2\text{C}\mathbf{1}]^{6+}$  were estimated (see Table 2). The  $K_a$  values for  $[\text{P}_0\text{C}\mathbf{1}]^{6+}$  and  $[\text{P}_1\text{C}\mathbf{1}]^{6+}$ , obtained by using UV/Vis spectroscopy, are consistent with the values estimated by using  $^1\text{H}$  NMR titrations.

A decrease in the stability of encapsulation is observed with an increase in the generation of the dendrimer precursor grafted onto the pyrenyl moiety. This can easily be understood since the pyrenyl part of the molecule is less accessible for encapsulation if it is attached to a higher generation. The association constants are quite high and the free energies ( $\Delta G^\circ$  up to  $-5.36\text{ kcal mol}^{-1}$ ) demonstrate a preference for the encapsulated system over the dissociated one, which is consistent with the DOSY measurements.

Pyrene has been intensively used as a fluorescent probe and its fluorescence is well documented.<sup>[25]</sup> Encapsulation of pyrene in metallaprism  $[\mathbf{1}]^{6+}$  quenches its fluorescence completely.<sup>[10b]</sup> Therefore, it is not surprising to observe quenching upon encapsulation of the pyrenyl moiety of the pyrenyl-containing dendrimers  $\text{P}_n$ . Spectral overlap between the emission of the pyrenyl moiety of  $\text{P}_0$  and the absorbance of the metallaprism  $[\mathbf{1}]^{6+}$  is observed (see Figure 5), which corresponds to an energy transfer effect between the pyrenyl moiety and the metallaprism.<sup>[26]</sup>

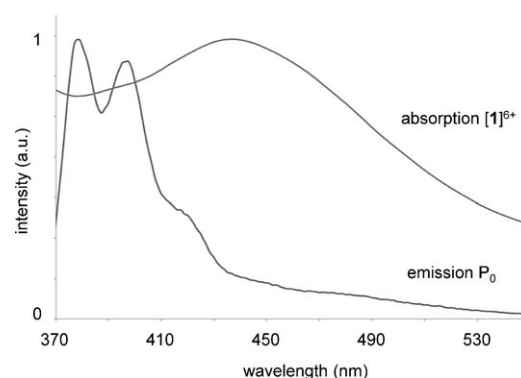


Figure 5. Normalised absorbance spectrum of metallaprism  $[\mathbf{1}]^{6+}$  and fluorescence spectrum of  $\text{P}_0$ .

As the guest molecule enters the cavity of the metallaprism there is a loss of excitation energy. Part of the energy is absorbed by the metallaprism, and consequently, the pyrenyl moiety encapsulated in the metallaprism is less excited and cannot re-emit the same energy as in the free state. This loss of excitation and energy transfer between the pyrenyl component and the metallaprism leads to a decrease in the emission energy of pyrene and ultimately to fluorescence quenching of the pyrenyl moiety.<sup>[27]</sup> Quenching of the fluorescence of pyrenyl-containing dendrimers in  $[\mathbf{1}]^{6+}$  is illustrated by the emission spectra from fluorescence titrations. Upon gradual addition of  $[\mathbf{1}][\text{CF}_3\text{SO}_3]_6$  (0.1–10.0 equiv) to a solution of  $\text{P}_0$  or  $\text{P}_1$  in  $\text{CH}_2\text{Cl}_2$  ( $10^{-7}\text{M}$ ), a strong quenching of the fluorescence is observed (see Figure 6 for the emission titration of  $\text{P}_0$ ).

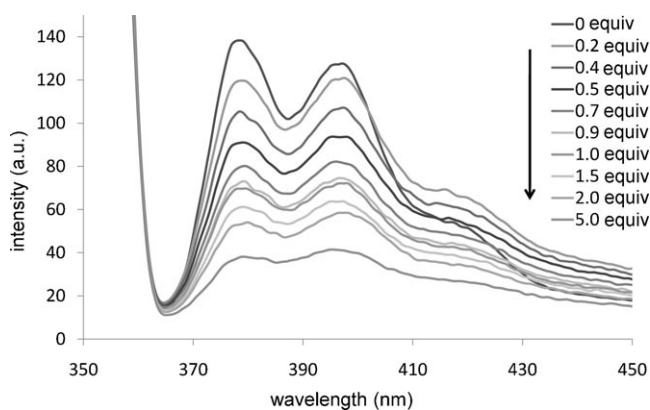


Figure 6. Fluorescence emission titration of  $[1]^{6+}$  in a solution of  $P_0$  in  $CH_2Cl_2$  ( $10^{-7} M$ ) at  $21^\circ C$ , with excitation at  $350 nm$ .

**Antiproliferative activity:** The antiproliferative activity of pyrenyl-containing dendrimers  $P_0$ ,  $P_1$  and  $P_2$ , the complex  $[1][CF_3SO_3]_6$  and the host–guest systems  $[P_n\subset 1][CF_3SO_3]_6$  were evaluated against the A2780 (cisplatin sensitive) and A2780cisR (cisplatin resistant) human ovarian cancer cell lines. Their cytotoxicities, in comparison to cisplatin, are presented in Table 3.

Table 3.  $IC_{50}$  values of pyrenyl-containing dendrimers  $P_0$ ,  $P_1$ ,  $P_2$  and complexes  $[1][CF_3SO_3]_6$  and  $[P_n\subset 1][CF_3SO_3]_6$  on A2780 and A2780cisR cell lines.

	A2780 ( $IC_{50}$ [ $\mu M$ ])	A2780cisR ( $IC_{50}$ [ $\mu M$ ])
$P_0$	inactive	inactive
$P_1$	inactive	inactive
$P_2$	inactive	inactive
$[1][CF_3SO_3]_6$	$3.1 \pm 1.0$	$4.6 \pm 0.5$
$[P_0\subset 1][CF_3SO_3]_6$	$0.4 \pm 0.1$	$0.5 \pm 0.4$
$[P_1\subset 1][CF_3SO_3]_6$	$2.2 \pm 1.1$	$2.4 \pm 0.8$
$[P_2\subset 1][CF_3SO_3]_6$	$2.6 \pm 0.8$	$2.8 \pm 1.0$
cisplatin	$1.6 \pm 0.6$	$8.6 \pm 0.6$

The pyrenyl-containing dendrimers  $P_0$ ,  $P_1$  and  $P_2$  are inactive against both A2780 and A2780cisR cancer cells, probably due to poor water solubility that results in their precipitation from the cell culture medium. The water-soluble metallaprism  $[1]^{6+}$  is quite cytotoxic and the host–guest systems are even more cytotoxic, in the case of  $[P_0\subset 1][CF_3SO_3]_6$  the  $IC_{50}$  value ( $0.4 \mu M$ ) shows it to be an order of magnitude more cytotoxic than the empty cage. The  $IC_{50}$  values of  $[P_1\subset 1][CF_3SO_3]_6$  and  $[P_2\subset 1][CF_3SO_3]_6$  are similar to those of the empty cage. High generations of dendritic systems are known to be biocompatible, and tend to show different levels of cytotoxicity,<sup>[28]</sup> however due to the lipophilic nature of  $P_n$ , their intrinsic cytotoxicity could not be established in this study. It is notable that  $[1]^{6+}$  and the host–guest systems show similar cytotoxicities for both the cisplatin-sensitive and cisplatin-resistant cancer cell lines, which indicates that they do not share the same mechanism of action as the reference drug, cisplatin.

To verify whether the host–guest systems remain intact before internalisation by the cancer cells, their stability was studied, by NMR spectroscopy, in  $D_2O$  and  $CD_3CN$  at room and elevated temperatures ( $> 50^\circ C$ ). These studies reveal that the host–guest compounds  $[P_n\subset 1]^{6+}$  are stable in solution for several hours. Moreover, upon addition of DMSO to the  $D_2O$  solution of  $[P_n\subset 1][CF_3SO_3]_6$ , no loss of the guest molecule was observed. Similarly, UV/Vis studies of the host–guest systems in the biological media at  $37^\circ C$  for 24 h show no spectral changes, thus confirming the strong encapsulation of the pyrenyl group within the cavity of  $[1]^{6+}$ . Consequently, the high stability of the host–guest systems suggests that intact  $[P_n\subset 1]^{6+}$  systems enter the cells.

## Conclusion

The synthesis of three new pyrenyl-containing dendrimers and their encapsulation into a water-soluble arene–ruthenium metallaprism is described. The host–guest systems,  $[P_n\subset 1][CF_3SO_3]_6$ , are remarkably stable in solution, as shown by NMR, UV/Vis and fluorescence spectroscopic studies. The cytotoxicity of the host–guest systems has been evaluated on human ovarian A2780 and A2780cisR cancer cell lines and an increase of one order of magnitude in cytotoxicity is observed for  $[P_0\subset 1][CF_3SO_3]_6$  compared with the empty metallaprism. The cytotoxicities of the higher generations of encapsulated dendrimers,  $[P_1\subset 1][CF_3SO_3]_6$  and  $[P_2\subset 1][CF_3SO_3]_6$ , were found to be equivalent to that of the cage alone. Notably, for the first time, this study has shown that metallacage host systems are able to deliver hydrophobic guest molecules with extremely large appendages into cancer cells.

## Acknowledgements

R.D. thanks the Swiss National Science Foundation (Grant No 200020-129501) for financial support. A generous loan of ruthenium chloride hydrate from the Johnson Matthey Technology Centre is gratefully acknowledged.

- [1] Y. Matsumura, H. Maeda, *Cancer Res.* **1986**, *46*, 6387–6392.
- [2] a) K. Iwai, H. Maeda, T. Konno, *Cancer Res.* **1984**, *44*, 2115–2121; b) K. Iwai, H. Maeda, T. Konno, Y. Matsumura, R. Yamashita, K. Yamasaki, S. Hirayama, Y. Miyauchi, *Anticancer Res.* **1987**, *7*, 321–327; c) T. Konno, H. Maeda, K. Iwai, S. Maki, S. Tashiro, M. Uchida, Y. Miyauchi, *Cancer* **1984**, *54*, 2367–2374; d) S. Maki, T. Konno, H. Maeda, *Cancer* **1985**, *56*, 751–757; e) T. Konno, H. Maeda, K. Iwai, S. Tashiro, S. Maki, T. Morinaga, M. Mochinaga, T. Hiraoka, I. Yokoyama, *Eur. J. Cancer Clin. Oncol.* **1983**, *19*, 1053–1065.
- [3] H. Maeda, *Adv. Enzyme Regul.* **2001**, *41*, 189–207.
- [4] J. Fang, H. Nakamura, A. K. Iyer, *J. Drug Targeting* **2007**, *15*, 475–486.
- [5] M. Yokoyama, T. Okano, Y. Sakurai, K. Kataoka, *J. Controlled Release* **1994**, *32*, 269–277.
- [6] R. Duncan, *Adv. Drug Delivery Rev.* **2009**, *61*, 1131–1148.
- [7] S. Zalipsky, M. Saad, R. Kiwan, E. Ber, N. Yu, T. Minko, *J. Drug Targeting* **2007**, *15*, 518–530.

- [8] a) N. T. Kimura, S. Taniguchi, K. Aoki, T. Baba, *Cancer Res.* **1980**, *40*, 2061–2068; b) M. Zhao, M. Yang, H. Ma, X. Li, X. Tan, S. Li, Z. Yang, R. M. Hoffman, *Cancer Res.* **2006**, *66*, 7647–7652.
- [9] B. Therrien, *Eur. J. Inorg. Chem.* **2009**, 2445–2453.
- [10] a) B. Therrien, G. Süss-Fink, P. Govindaswamy, A. K. Renfrew, P. J. Dyson, *Angew. Chem.* **2008**, *120*, 3833–3836; *Angew. Chem. Int. Ed.* **2008**, *47*, 3773–3776; b) O. Zava, J. Mattsson, B. Therrien, P. J. Dyson, *Chem. Eur. J.* **2010**, *16*, 1428–1431.
- [11] a) J. Mattsson, P. Govindaswamy, J. Furrer, Y. Sei, K. Yamaguchi, G. Süss-Fink, B. Therrien, *Organometallics* **2008**, *27*, 4346–4356; b) J. Mattsson, O. Zava, A. K. Renfrew, Y. Sei, K. Yamaguchi, P. J. Dyson, B. Therrien, *Dalton Trans.* **2010**, 39, 8248–8255.
- [12] a) N. P. E. Barry, B. Therrien, *Eur. J. Inorg. Chem.* **2009**, 4695–4700; b) J. Freudenreich, N. P. E. Barry, G. Süss-Fink, B. Therrien, *Eur. J. Inorg. Chem.* **2010**, 2400–2405.
- [13] a) J. Mattsson, P. Govindaswamy, A. K. Renfrew, P. J. Dyson, P. Štěpnička, G. Süss-Fink, B. Therrien, *Organometallics* **2009**, *28*, 4350–4357; b) F. Linares, E. Quartapelle Procopio, M. A. Galindo, M. Angustias Romero, J. A. R. Navarro, E. Barea, *CrystEngComm* **2010**, *12*, 2343–2346.
- [14] a) F. Linares, M. A. Galindo, S. Galli, M. Angustias Romero, J. A. R. Navarro, E. Barea, *Inorg. Chem.* **2009**, *48*, 7413–7420; b) N. P. E. Barry, J. Furrer, B. Therrien, *Helv. Chim. Acta* **2010**, *93*, 1313–1328.
- [15] N. P. E. Barry, O. Zava, P. J. Dyson, B. Therrien, *Aust. J. Chem.* **2010**, *63*, 1529–1537.
- [16] B. Dardel, D. Guillon, B. Heinrich, R. Deschenaux, *J. Mater. Chem.* **2001**, *11*, 2814–2831.
- [17] R. Deschenaux, B. Donnio, D. Guillon, *New J. Chem.* **2007**, *31*, 1064–1073.
- [18] a) D. H. Wu, A. Chen, C. S. Johnson, Jr., *J. Magn. Reson. A.* **1995**, *115*, 123–126; b) C. S. Johnson, Jr., *Prog. Nucl. Magn. Reson. Spectrosc.* **1999**, *34*, 203–256; c) D. Ajami, J. Rebek, Jr., *Angew. Chem.* **2007**, *119*, 9443–9446; *Angew. Chem. Int. Ed.* **2007**, *46*, 9283–9286; d) J.-F. Lemonnier, S. Floquet, A. Kachmar, M.-M. Rohmer, M. Bénard, J. Marrot, E. Terazzi, C. Piguet, E. Cadot, *Dalton Trans.* **2007**, 3043–3054; e) N. P. E. Barry, J. Furrer, J. Freudenreich, G. Süss-Fink, B. Therrien, *Eur. J. Inorg. Chem.* **2010**, 725–728.
- [19] a) D. Li, G. Kagan, R. Hopson, P. G. Williard, *J. Am. Chem. Soc.* **2009**, *131*, 5627–5634; b) A. Macchioni, G. Ciancaleoni, C. Zuccaccia, D. Zuccaccia, *Chem. Soc. Rev.* **2008**, *37*, 479–489.
- [20] a) M. K. Dymond, G. S. Attard, *Langmuir* **2008**, *24*, 11743–11751; b) S. R. Meyers, F. S. Juhn, A. P. Griset, N. R. Luman, M. W. Grinstaff, *J. Am. Chem. Soc.* **2008**, *130*, 14444–14445; c) S. Chen, X.-Z. Zhang, S.-X. Cheng, R.-X. Zhuo, Z.-W. Gu, *Biomacromolecules* **2008**, *9*, 2578–2585; d) V. Percec, D. A. Wilson, P. Leowanawat, C. J. Wilson, A. D. Hughes, M. S. Kaucher, D. A. Hammer, D. H. Levine, A. J. Kim, F. S. Bates, K. P. Davis, T. P. Lodge, M. L. Klein, R. H. De Vane, E. Aqad, B. M. Rosen, A. O. Argintaru, M. J. Sienkowska, K. Rissanen, S. Nummelin, J. Ropponen, *Science* **2010**, *328*, 1009–1014.
- [21] a) Y. Kikuchi, Y. Kato, Y. Tanaka, H. Toi, Y. Aoyama, *J. Am. Chem. Soc.* **1991**, *113*, 1349–1354; b) L. Fielding, *Tetrahedron* **2000**, *56*, 6151–6170.
- [22] M. J. Hynes, *J. Chem. Soc. Dalton Trans.* **1993**, 311–312.
- [23] Y. Tsukube, H. Furuta, A. Odani, Y. Takeda, Y. Kudo, Y. Inoue, Y. Liu, H. Sakamoto, K. Kimura in *Comprehensive Supramolecular Chemistry* (Eds.: J. L. Atwood, J. E. D. Davies, D. D. Macnicol, F. Vögtle), Pergamon Press, Oxford, **1996**, pp. 425–482.
- [24] K. A. Connors *Binding Constants*, Wiley, New York, **1987**, pp. 141–187.
- [25] F. Ariese, A. N. Bader, C. Gooijer, *TrAC Trends Anal. Chem.* **2008**, *27*, 127–138.
- [26] a) C. Wu, Y. Zheng, C. Szymanski, J. McNeill, *J. Phys. Chem. C* **2008**, *112*, 1772–1781; b) M. J. Aguirre, E. A. Lissi, A. F. Olea, *J. Photochem.* **1987**, *36*, 177–184.
- [27] N. Bouquin, V. L. Malinovsky, R. Häner, *Chem. Commun.* **2008**, 1974–1976.
- [28] a) R. Duncan, L. Izzo, *Adv. Drug Delivery Rev.* **2005**, *57*, 2215–2237; b) A. Samad, I. Alam, K. Saxena, *Curr. Pharm. Des.* **2009**, *15*, 2958–2969; c) K. Jaina, P. Kesharwanja, U. Gupta, N. K. Jain, *Int. J. Pharm.* **2010**, *394*, 122–142; d) J. La Rocque, D. J. Bharali, S. A. Mousa, *Mol. Biotechnol.* **2009**, *42*, 358–366; e) M. Labieniec, O. Ulicna, O. Vancova, J. Kucharska, T. Gabryelak, C. Watala, *Cell Biol. Int.* **2010**, *34*, 89–97; f) S. Svenson, *Eur. J. Pharm. Biopharm.* **2009**, *71*, 445–462.
- [29] Hyperchem Computational Chemistry Software Package Version 7.5, Hypercube Inc., Gainesville, Florida (**2003**).

Received: September 13, 2010  
Published online: January 5, 2011